Received November 25, 2019, accepted December 6, 2019, date of publication January 6, 2020, date of current version January 9, 2020.

Digital Object Identifier 10.1109/ACCESS.2019.2963227

Rejuvenation of Retired Power Cables by Heat Treatment: Experimental Simulation in Lab

YUE XIE[1], (Student Member, IEEE), YIFENG ZHAO[1], SHUZHEN BAO[1], PENGYU WANG[1], JIASHENG HUANG[2], GANG LIU[1], YANPENG HAO[1], (Member, IEEE), AND LICHENG LI[1]

[1]School of Electric Power, South China University of Technology, Guangzhou 510630, China
[2]Transmission management office, Guangzhou Power Supply Bureau, Guangzhou 510640, China

Corresponding authors: Gang Liu (liugang@scut.edu.cn) and Yanpeng Hao (yphao@scut.edu.cn)

ABSTRACT In this work, heat treatment was performed on three retired 110 kV AC cables with service years of 0, 15 and 30, and the effects on the thermal and electrical performance of the cable insulation were investigated. First, each cable with a length approximately of 5 m was prepared and cut into five equal segments. Four segments of each cable were annealed at a temperature of 90, 95, 100, or 105 °C by building a small circuit to simulate cable operation. Then, a section at the middle of each segment was cut out, and the insulation layer was peeled away. The peeled-off layers from the inner, middle and outer positions were selected as the test samples. Subsequently, Fourier transform infrared spectrometry (FTIR), and differential scanning calorimetry (DSC) were performed, and the DC conduction current and dielectric breakdown strength were measured. The best thermal properties of the highest melting point, crystallinity, and smallest melting range were found when the cables were annealed at 100, 105, and 105 °C for the inner, middle, and outer positions, respectively. The highest dielectric breakdown strength and lowest electrical conductivity were found at temperatures of 95 or 100 °C for the inner and middle positions, respectively, and at 105 °C for the outer position. The FTIR results showed that thermal annealing for hundreds of hours did not adversely affect the molecular chains. It is found that this type of heat treatment could be a feasible method to rejuvenate retired cables, and a conservative temperature of 95 °C is regarded as the optimum annealing temperature.

INDEX TERMS Cable, DSC, melting point, crystallinity, electrical conductivity, dielectric breakdown strength.

I. INTRODUCTION

Cross-linked polyethylene (XLPE) is widely used as an insulation material in high-voltage cables due to its excellent electrical properties [1]. During cable operation, insulation degradation severely threatens the safety of cable operation, and this problem has prompted widespread concern. Generally, the service years is limited to 30 years for most 110 kV cables under the condition that the temperature in the metal conductor does not exceed 90 °C. In most cases, cables operate under mild conditions with relatively low current and temperature in the insulation layer unless some emergency occurs. Many studies have reported that retired cables retain good electrical properties and some of them remain to meet the standards of cable operation, although they have reached the designed service year and suffered insulation degradation [2], [3]. As insulation degradation becomes more severe, the probability of an insulation failure accident increases. In this case, one problem raised for those cables that have reached the designed service year: continue operation or replaced by new cables? Although many detection technologies have been developed, such as the detection of partial discharge, damped oscillation waves, and time-frequency reflection, the accuracy of these measurements is still lacking because of the multiple interferences from other cables and the complex on-site environment [4]–[6]. Until now, a feasible method for the accurate assessment of insulation degradation that is conducive to the evaluation of cable retirement was not currently available.

XLPE is a typical semi-crystalline polymer whose temperature-sensitive microstructure dominates its thermal

The associate editor coordinating the review of this manuscript and approving it for publication was Boxue Du.

TABLE 1. Important specifications of selected three cables.

Sample	M_I	M_C	d_{IS}	d_I	d_{OC}	S_C	O_P
S1	XLPE	Cu	2	19.8	2	700	-
S2	XLPE	Cu	2	19.8	2	700	2000-2015
S3	XLPE	Cu	2	19.8	2	700	1985-2015

M_I: insulation material, M_C: conductor material, d_{IS}: inner semiconductor thickness in mm, d_I: insulation thickness in mm, d_{OC}: outer semiconductor thickness in mm, S_C: conductor area in mm^2, O_P: operation period. Other parameters such as cross-linking method are unknown.

and electrical properties [7]. For commercial XLPE cables, the microstructure of XLPE can't reach a thermodynamic equilibrium state in the short period of the manufacturing process [8]. Many studies on retired cables that operated for decades have revealed a phenomenon in which many retired cables maintain better thermal and electrical properties than new cables [9], [10], because the cables have gone through an annealing process during cable operation with elevated temperatures promoted molecular chain movement and favor the emergence and growth of new crystals and the rearrangement of the crystal-amorphous region [9]–[11]. In our previous research, thermal annealing was performed on XLPE sheets peeled from retired cables at the temperatures around 90 °C; the results showed that the thermal and electrical properties were significantly enhanced by the heat treatment, and 95 °C exhibits the best results [12], [13]. These studies provide the possibility that the XLPE from retired cables could be rejuvenated. When the cable is in operation, the enhanced thermal and electrical properties of cable insulation ensure a relatively low failure rate and long service year. However, the annealing process is not consistent with the actual environment of cable operation, and the previous results did not sufficiently support the use of this treatment in a real cable line [14].

In the present study, thermal annealing was performed on three retired cables that had operated for 0, 15, and 30 years. The heat treatment was performed by building a small circuit to simulate cable operation. The effects on the cable, including the changes in the thermal and electrical performance at different positions of the insulation layer were analyzed, and the feasibility of cable rejuvenation by heat treatment was discussed.

II. EXPERIMENTAL SETTING AND SAMPLE PREPARATION

A. CABLE DESCRIPTION

Three cables were used in this study; two of them were retired cables with a service year of 15 and 30 years, and the other cable was a spare cable. They came from different manufacturers and differed from the cables used in [12]. The two retired cables were in good condition when they were out of service because of the movement of the cable transmission line. No physical damage was found on the surface of the outer aluminum sheath. No overheated operation was reported for the two retired cables, which means the temperature in the insulation layer was always below 90 °C during the long-term cable operation.

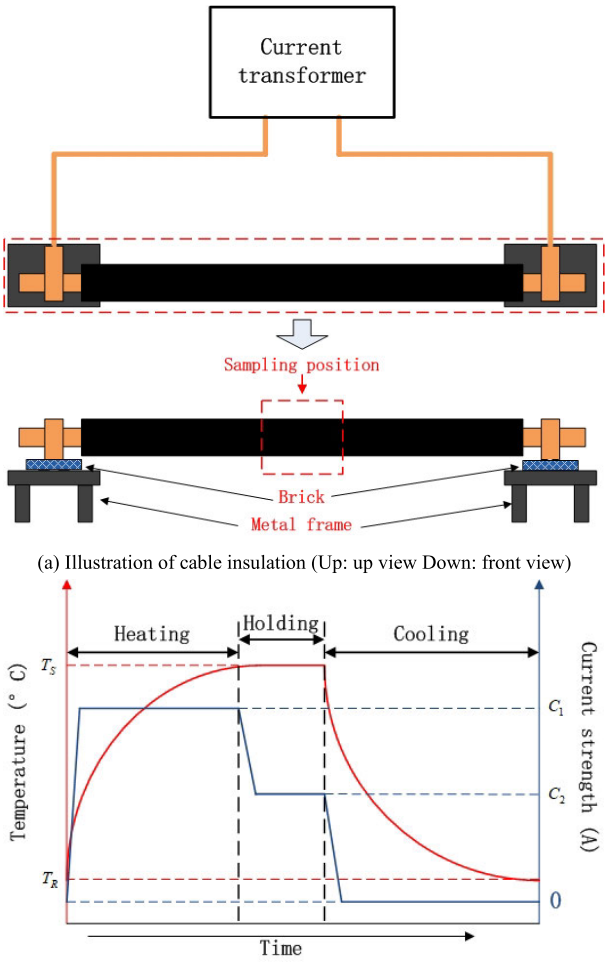

FIGURE 1. Schematic graph of cable installation. T_R: room temperature, T_S: preset temperature, C_1: applied current 1, C_2: applied current 2.

Each cable, with a length of 5 m, was prepared and cut into five equal segments. The outer sheath and insulation layer at the both ends of each segment approximately 15 cm was peeled, and the metal conductor was exposed.

B. EXPERIMENTAL SETTING

As illustrated in Figure 1(a), one segment was connected to a current generator (AHY-3000, IUXPOWER, China) with copper connectors, and placed on metal frames. Figure 1(b) exhibits the process map of synchronous changes in the temperature and the strength of the applied current. In the heating phase, a large current of C_1 was applied to the cable, Joule heat produced in the inner conductor, and lead to the temperature increases from room temperature to the preset temperature in 12 hours. Then, the applied current decreases to a small value of C_2, balance the heat production and dissipation, the temperature holding at the preset temperature for 2 hours. Finally, the current decreases to 0, the cable naturally

TABLE 2. Important paeameters for heat treatment.

T_{pre}(°C)	t_h(h)	t_c(h)	C_1(A)	C_2(A)
90	12	14.3	1200	1060
95	12	15.9	1240	1090
100	12	17.1	1280	1110
105	12	17.6	1310	1150

t_h: heating time, t_c: cooling time, C_1: current in heating phase, C_2: current in holding phase.

TABLE 3. Temperature distribution in different positions at different preset temperatures.

T_s	T_{out}	T_{mid}	T_{inn}
90	80.6	82.6	89.3
95	85.4	88.6	94.1
100	88.3	92	99.0
105	93.8	97	104.1

T_s: preset temperature, same as the conductor temperature, T_{out}: temperature in outer position, T_{mid}: temperature in middle position, T_{inner}: temperature in inner position.

cooled to room temperature. Such a consecutive heating, holding, and cooling phase constitute a thermal cycle; the same cycle was repeated 20 times for each segment. Each cable was annealed at four preset temperatures of 90, 95, 100, and 105 °C, corresponding to the four segments of each cable, with one segment is annealed at one preset point. The last one segment without annealing is regarded as the fresh sample.

Before the heat treatment, the strength of the applied current in heating and holding phase and the time duration in the heating and cooling phase at different preset temperatures were measured experimentally, the results are summarized in Table 2.

C. TEMPERATURE DISTRIBUTION

During the measurement of the parameters shown in Table 2, the maximum temperature at the three positions at different preset temperatures were recorded and are summarized in Table 3. Joule heat produced in the inner conductor and is transferred outwards, producing a temperature gradient distributed across the insulation. It is clearly seen from the Table 3 that the highest temperature always appears at the inner position and is only about 1 °C lower than that of the preset point, and the lowest temperature always appears at the outer position. As the preset annealing temperature increases to 105 °C, the difference between T_{pre} and T_{out} increases from 9.2 to 12.3 °C.

D. SAMPLE PREPARATION

When the heat treatment process was finished, a short section of 15 cm at the middle of each segment was cut to get the test cable, as shown in Figure 1(a).

During the measurement of the parameters shown in Table

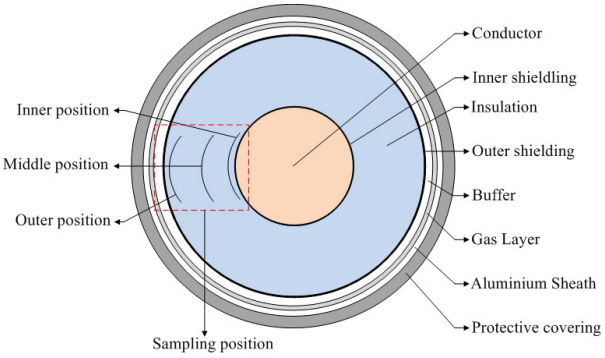

(a) Illustration of sampling position

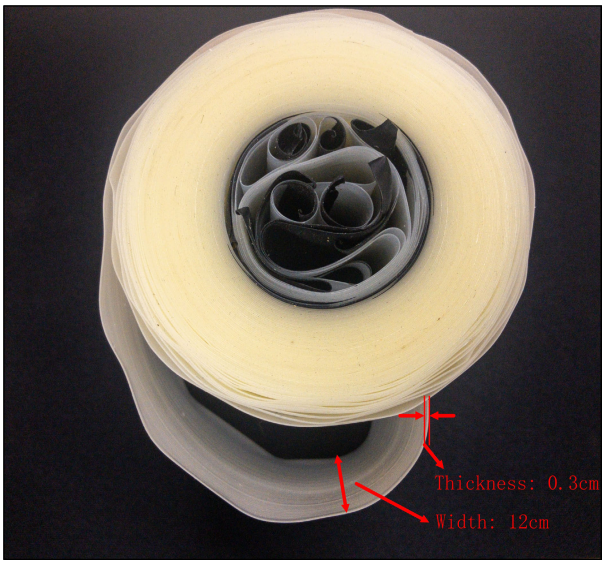

(b) Type-like XLPE peels obtained

FIGURE 2. Diagram of sampling position in the cable insulation layer.

To investigate the annealing effects on the cable insulation, the XLPE from three different positions of the insulation layer was selected to represent the whole insulation layer. The outer sheath of the test cable was removed, the cable insulation was peeled along the surface of the inner conductor, and tape-like peels were obtained, as shown in Figure 2(b). As illustrated in Figure 2(a), three positions located from the inner semi-conductive layer to the outer semi-conductive layer of the insulation layer were selected. The XLPE peels from the same cable were named depending on their locations in the insulation layer: inner, middle, and outer position; and the peels from different cables were named according to their service year: XLPE-0, XLPE-15, and XLPE-30.

E. MEASUREMENT

The change in molecular chain was investigated by the measurement of the Fourier Transform Infrared Spectroscopy (FTIR) on a Bruker 77 (Bruker, Germany). The wavelength scanning range is 400 $\sim$ 4000 cm^{-1}, with a resolution of 4 cm^{-1}. Five repeated scanning for each sample was

performed to increase the accuracy, and the displayed spectra was the averages of the five repeated scanning spectra.

The thermal performance was manifested by the measurement of the differential scanning calorimetry (DSC), which is carried out on a Q200 (DSC, TA Instruments). The sample with a weight of 5mg was tested in each measurement. The sample was first heated from 25 to 140 °C at a rate of 10 °C/min, and kept for 5 min. Then cooled to 25 °C at a rate of −10 °C/min. The same scanning was repeated twice.

The electrical performance was investigated by the measurement of the DC conduction current and dielectric breakdown strength E_B. The DC conduction current was measured at 90 °C by a three-electrode measurement instrument with an electrometer (Keithely 6517B, Tektronix, USA). The electric field of 20 kV/mm was applied and the current was recorded for 3600 s. The average of the last 30 s was calculated as the valid current. The dielectric breakdown strength E_B was measured at the same temperature as the DC conduction current. A pair of copper plate electrode was used, the sample was inserted between the two electrodes and they were totally immersed in the silicone oil. The AC (50 Hz) voltages were applied to the electrodes, the voltage increased linearly at a speed of 1 kV/s until to the sample breakdown occurred. Same measurement was repeated 15 times, the average and deviation were calculated.

III. RESULTS AND DISCUSSION

A. ANNEALING EFFECT ON THERMAL PERFORMANCE

Due to the large amount of DSC data measured for all samples, only the data of XLPE-30 and XLPE-15 are presented, as shown in the following figures.

Figure 3 shows the melting endotherms observed for the two cables measured in the first heating phase. In each graph of Figure 3(a), a low-temperature melting peak appears, as the cable was annealed at 90 °C. As the annealing temperature increases, the low-temperature melting peak shifts to a higher temperature and the melting range becomes narrower, while no change appears in the main melting peak. This result means that the thinner lamellae emerged and recrystallized to thicker lamellae as the annealing temperature increased [15]. When the cable was annealed at 100 °C, the low-temperature melting peak overlapped with the main melting peak. Simultaneously, the melting peak became a pointed shape and shifted to a higher temperature. This result occurred because the thin lamellae grew to thicker lamellae, and the thickness approach that of the original lamellae; in addition, the original lamellae corresponding to the melting point were further thickened [16]. When the cable was annealed at a higher temperature of 105 °C, the main melting peak shifted to a lower temperature, and the melting range became broader with the reappearance of the low-temperature melting peak. This effect is caused by the melting of thicker lamellae and the re-emergence of the thin lamellae [17]. In Figure 3(b), a similar phenomenon is observed: the low-temperature melting peak appears when the cable was annealed at 90 °C and

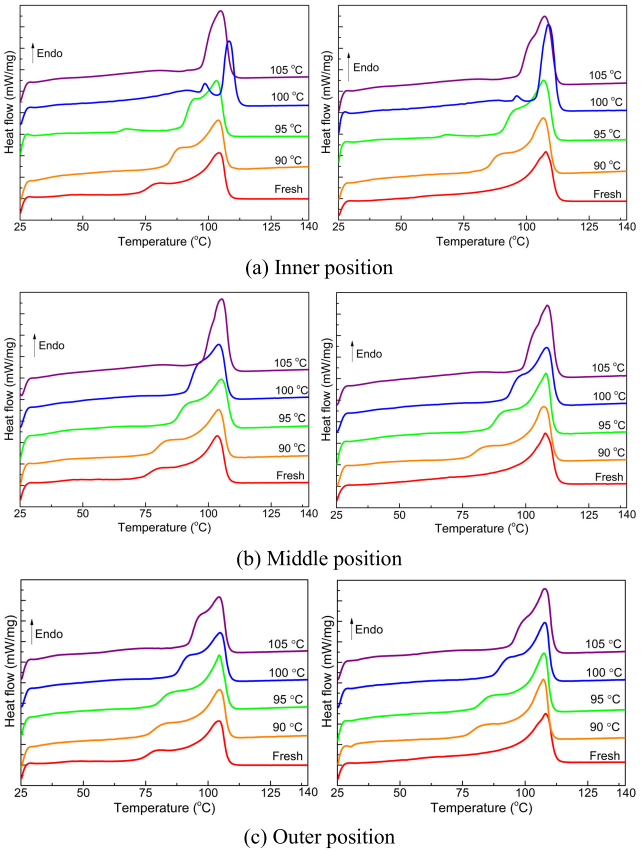

FIGURE 3. Melting endotherms measured in the first heating phase. Left is XLPE-15, right is XLPE-30.

shifts to a higher temperature as the annealing temperature increases. When the cables were annealed at 105 °C, the melting range becomes the most narrow with the overlap of the two melting peaks and slightly shifts to a higher temperature. However, the behavior not strictly the same as that of the inner position at the annealing temperature of 100°C. In Figure 3(c), the low-temperature melting peak appears as the cable was annealed at 90 °C and shifts to high temperatures as the annealing temperature increases. The two melting peaks partly overlap with a distinct distance, and no change in the main melting peak even at the highest annealing temperature of 105 °C.

Generally, the melting endotherms in the second heating phase are also highly important. Figure 4 shows the melting endotherms observed for XLPE-30 and XLPE-15 measured in the second heating phase. In each graph of the part (a), (b) and (c), the five melting curves show almost the same melting point and endotherms at each temperature, which means that a similar crystal structure emerged in the first cooling phase [18]. All crystals were melted when the sample was heated to 140 °C in the first heating phase and recrystallized in the first cooling phase. Under the measurement conditions of the same cooling rate and temperature range, the emergence of a similar crystal structure indicates that the heat treatment at different temperatures did not further damage the molecular chain [19].

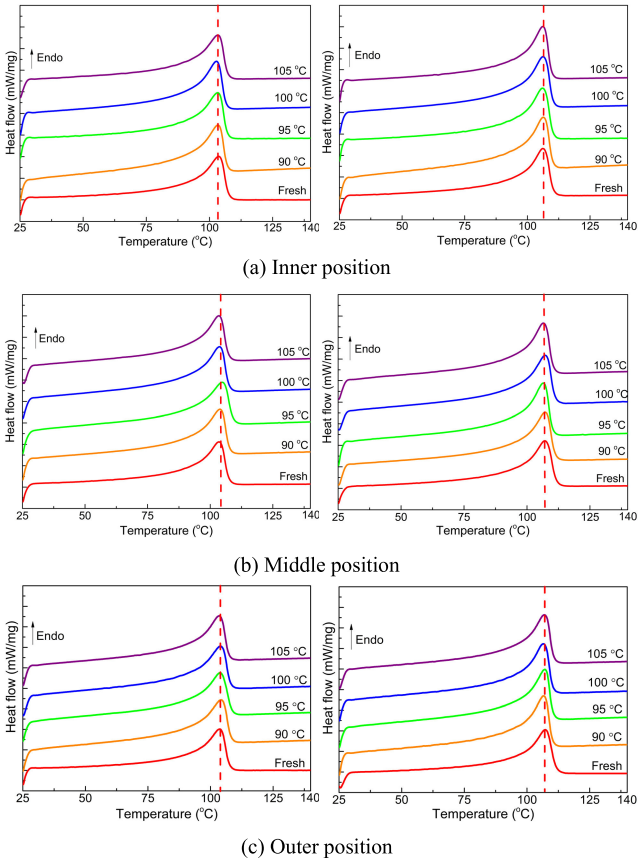

FIGURE 4. **Melting endotherms measured in the second heating phase for XLPE-15 and XLPE-30. Left is XLPE-15, right is XLPE-30.**

A comparing of the melting endotherms measured in the first and the second heating phases shown in Figures 3 and 4 indicates that the DSC spectra measured in the first heating phase provide useful information about the annealing effect on the changes in thermal properties.

Based on the melting curves measured in the first heating phase, the crystallinity and melting range are calculated by using the following two equations [12], [20],

$$\mathrm{X} = \frac{\Delta H_0}{\Delta H_m} \times 100\% \tag{1}$$

$$\Delta \mathrm{T} = T_{mi} - T_{me} \tag{2}$$

where ΔH_{o} is the fusion enthalpy per unit volume observed and ΔH_{m} is the corresponding value of an ideal polyethylene crystal, $2.88\times10^{8}\mathrm{J\cdot m^{-3}}$. T_{mi} is the initial melting point, and T_{me} is the ending melting point.

Figure 5 shows the values of the crystallinity and melting range observed for all samples. It is seen that the X increases and ΔT decreases as the annealing temperature increases, reaching the optimum values at annealing temperatures of 100, 105, and 105 °C, corresponding to the inner, middle, and outer positions, respectively. Note that the lamellae structure is the basic unit of the crystal, the emergence and growth of thin lamellae and the thickness approach those of the original lamellae, leading to a smaller melting range

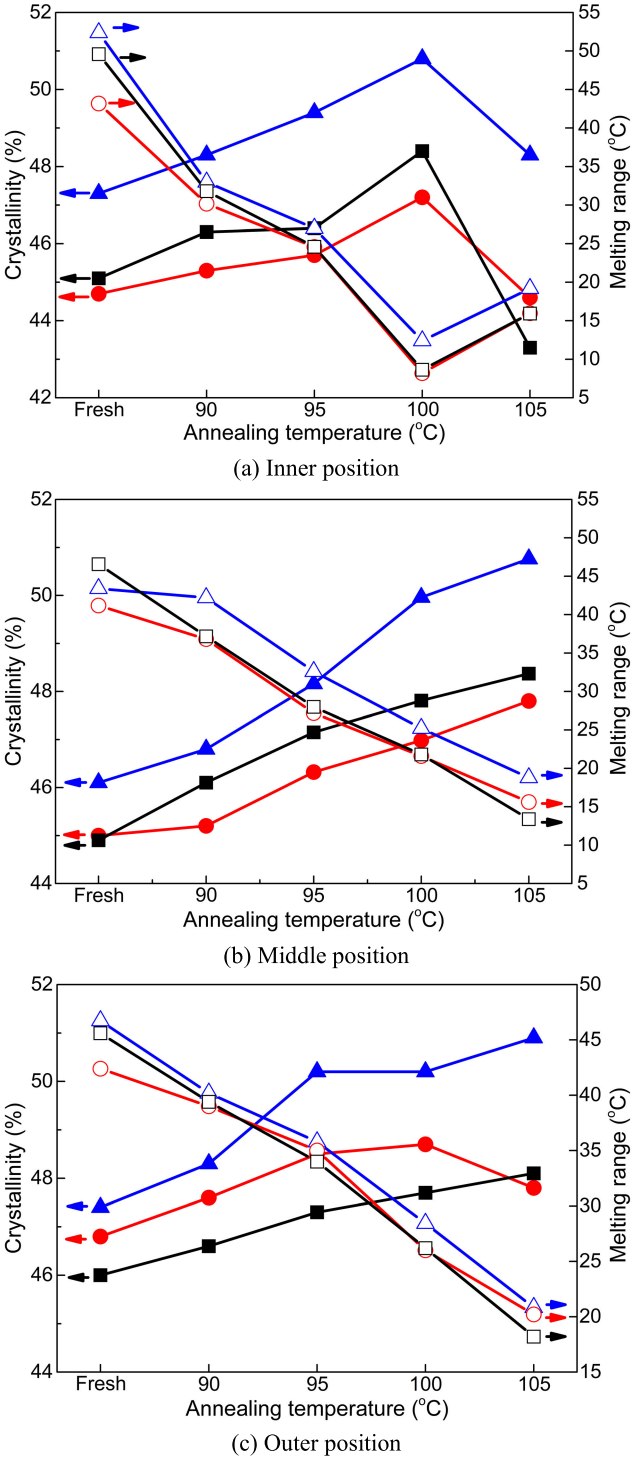

FIGURE 5. **Crystallinity and melting range as a function of annealing temperature. Solid symbols (■, ●, ▲) represent crystallinity of XLPE-0, XLPE-15, and XLPE-30, Open symbols (□, ○, △) represent melting range of XLPE-0, XLPE-15, and XLPE-30.**

and favoring the enlargement of the crystal region, so that the changes in these two factors show the same trend as the changes in the melting curves shown in Figure 3 [21].

To investigate the change in the melting curve during the annealing process, the two melting peaks were separated

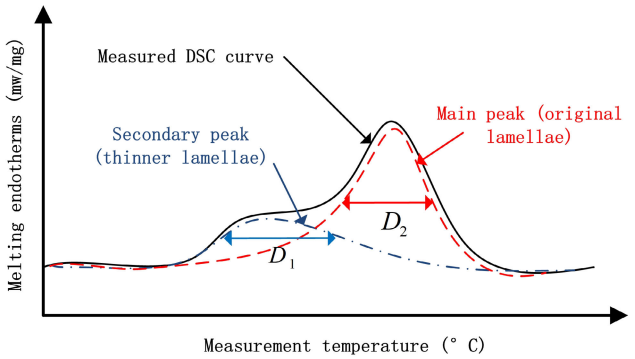

FIGURE 6. Diagram of peak separation and fitting for DSC melting curve.

by the Gauss peak fitting function in Origin 9.1, and the diagram of the separation results is shown in Figure 6. The main melting peak and the low-temperature melting peak represent the original lamellae and the new thinner lamellae, respectively; in other words, the changes in the two melting peaks correspond to the changes in the distribution of the crystal size. The half peak widths for the two melting peaks were calculated through the fitting works.

As shown in Figure 7, D1 and D2 first decrease as the annealing temperature increases, and the smallest values are observed at the inner, middle, and outer positions of the cables at the annealing temperatures 100, 105, and 105 °C. Importantly, as shown in Figure 3, no low-temperature melting peak was observed in the three positions of XLPE-30 before annealing, so that the valued of D1 for the fresh sample is absent. The decreases in D1 and D2 means relatively uniform distribution of the lamellar thickness for the two different lamellae. This result indicates that the thermal annealing process contributes to denser distribution of crystal region, this change has been shown to the improving thermal and electrical performance [22].

As illustrated in Tabl 2, the actual temperature at the inner position is 99 °C at an annealing temperature of 100 °C, and the changes in the factors of thermal performance indicate the existence of an optimum annealing point or range. Although the middle position shows the best thermal performance (with an actual temperature of 97 °C at an annealing point of 105 °C), as with the inner position, the optimum annealing point cannot be entirely confirmed unless the heat treatment is conducted at higher temperatures. Apparently, the actual temperature at the outer position is 94 °C at an annealing temperature of 105 °C, which is obviously below the optimum annealing point deduced from the inner position, so this region does do not show the best thermal performance.

For a commercial cable, more attention should be paid to the inner position because this position was exposed to the severest thermal and electrical stresses during the cable operation, and easily cause insulation degradation. As shown in Figures 4 and 6, 100 °C gives the best results of the thermal performance for the inner position, with significant

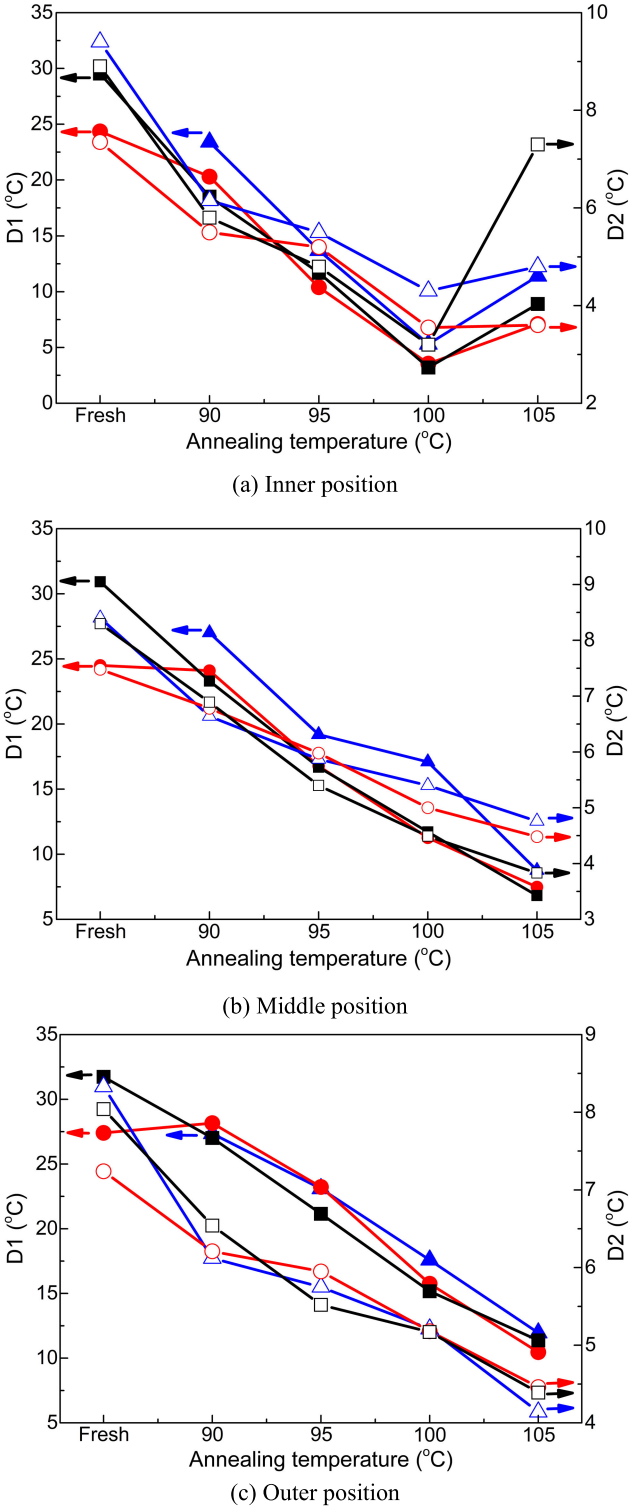

FIGURE 7. D1 and D2 as a function of annealing temperature. Solid symbols (■, ●, ▲) represent D1 of XLPE-0, XLPE-15, and XLPE-30, Open symbols (□, ○, △) represent D2 of XLPE-0, XLPE-15, and XLPE-30.

enhancement at the middle and outer positions. In this case, 100 °C is regarded as the optimum annealing temperature in terms of the coaxial configuration of the cable.

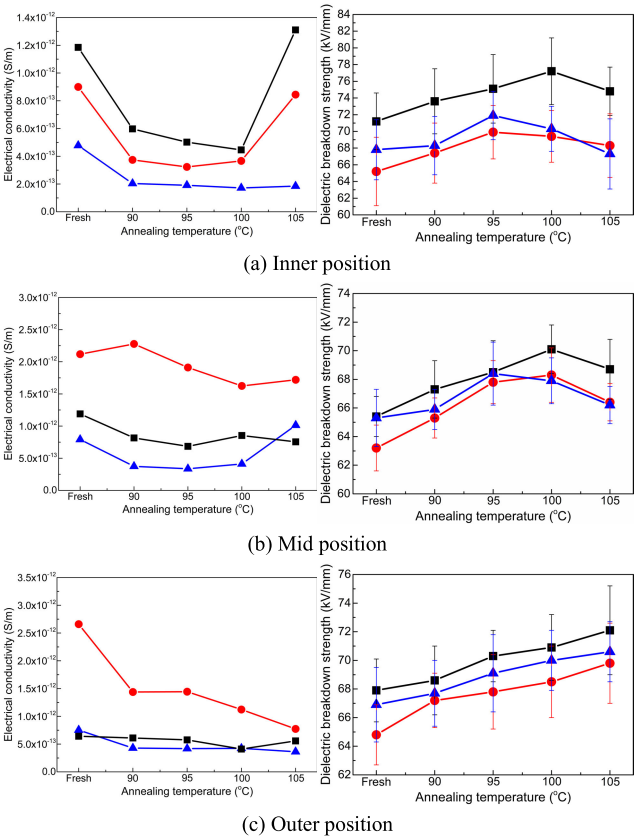

(a) Inner position

(b) Mid position

(c) Outer position

FIGURE 8. Electrical conductivity σ_{DC} and dielectric breakdown strength E_B as a function of annealing temperature. XLPE-0 (■), XLPE-15 (●), XLPE-30 (▲).

B. ANNEALING EFFECT ON ELECTRICAL PERFORMANCE

Based on the measured DC conduction current, the electrical conductivity σ_{DC} was calculated using the equation [23]:

$$\sigma_{DC} = \frac{I}{SE} \tag{3}$$

where I_{av} is the average DC conduction current in the last 60 s, S is the area of the electrode, and E is the strength of the applied electric field.

Figure 8 shows the values of σ_{DC} and E_B as a function of annealing temperature. At the outer position, σ_{DC} and E_B of the three cables monotonically change as the annealing temperature increases, reaching the optimum values at the same annealing temperature of 105 °C. At the inner position, σ_{DC} of the three cables first decreases as the annealing temperature increases, XLPE-0 and XLPE-30 show the smallest σ_{DC} at the an temperature of 100 °C, and XLPE-15 shows the minimum at 95 °C. E_B of the three cables increases as the annealing temperature increases, XLPE-15 and XLPE-30 reach the highest E_B at an annealing temperature of 95 °C, and XLPE-0 reaches the highest E_B at a higher temperature of 100 °C. At the middle position, XLPE-15 shows the smallest σ_{DC} at an annealing temperature of 100 °C; the other two cables show the smallest σ_{DC} at the lower temperature of 95 °C, almost identical to the values at 100 °C; and the highest E_B is observed at annealing temperatures of 95, 95, 100 °C for XLPE-15, XLPE-30, and XLPE-0, respectively. It is widely accepted that charge transport is harder in crystal regions and easier in amorphous regions [24]. New lamellae emerge and grow, which is beneficial to thicker lamellae and higher crystallinity. Moreover, a higher annealing temperature promotes a uniform molecular chain arrangement, favoring the elimination of defects [25]. In this case, the annealing temperature dependence of σ_{DC} and E_B shows a similar trend as the DSC results. However, the inner and middle positions, the optimum point of electrical performance is below the optimum point of thermal performance. For example, the three cables exhibit the best values of σ_{DC} and E_B at annealing temperatures of 95 or 100 °C, while the best values of thermal performance appear at 100 and 105 °C at the inner and middle position. The reason seems to be that the ionization of impurities contributes to the concentration of charge carriers.

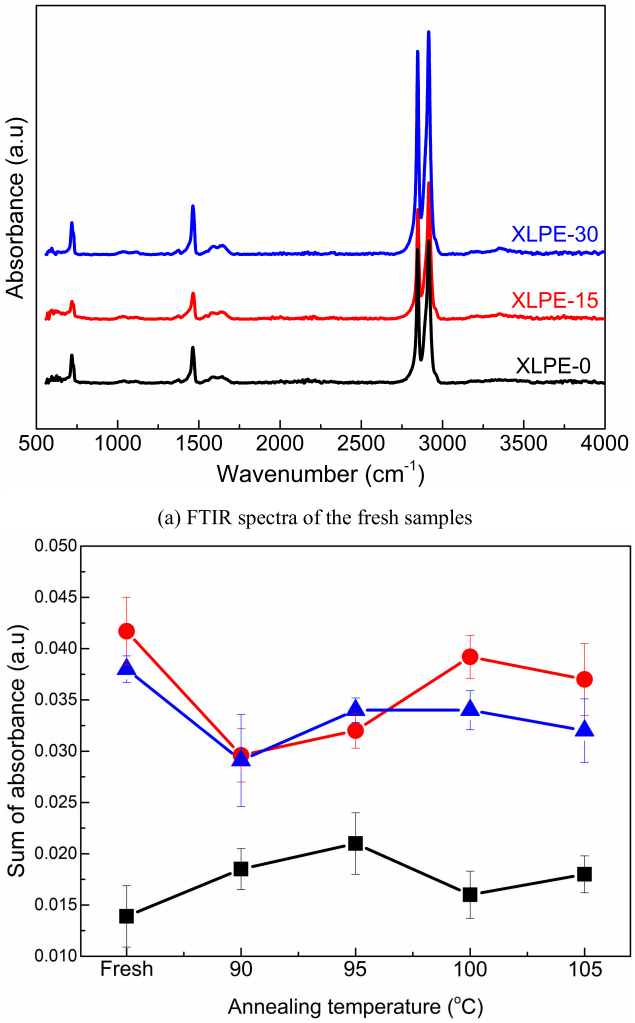

(a) FTIR spectra of the fresh samples

(b) Sum of the absorbance

FIGURE 9. FTIR results. ■ : XLPE-0, ●: XLPE-15, ▲: XLPE-30.

In summary, the three positions of cables show the best thermal and electrical performance at different temperatures. Concerning the electrical performance, 95 °C is the optimum annealing point for XLPE-15 and XLPE-30, 100 °C would be the optimum point for XLPE-0. In consideration of the annealing effects on the thermal and electrical performance, a conservative temperature of 95 °C is considered the optimum point.

C. ANNEALING EFFECTS ON THE MOLECULAR CHAIN DAMAGE

Figure 9 shows FTIR absorbance results. Figure 9(a) shows the spectra of the fresh samples from the inner positions. The absorbance peaks at 1635, 1741, and 3359 cm^{-1} corresponding to the double bond, carbonyl group, and hydroxy group, respectively, are the most distinctive features of cable insulation degradation, are selected to evaluate the molecular chain damage [26]. For that case, the sum of the absorbance of the three groups is calculated, to represent the molecular chain damage.

Figure 9(b) shows the sum of absorbance strength as a function of annealing temperature. It is clearly seen that XLPE-15 and XLPE-30 show higher absorbance than XLPE-0, which means that severe insulation degradation has occurred in the two retired cables. After the cables were annealed at different temperatures, slight changes were observed in each position, with only minuscule fluctuations, which could be attribute to the difference in the chemical group distribution. It is inferred that the thermal annealing process did not result in further damage to the molecular chain. This outcome is consistent with the conclusions mentioned in Figure 4(b) that a similar molecular chain is beneficial for a similar crystal-amorphous structure under the same conditions.

IV. CONCLUSION

Thermal annealing was performed on three cables with service year of 0, 15, and 30 years. The effects on the thermal and electrical properties at three different positions in the cable insulation were investigated experimentally. In summary, the following findings are presented:

1) The optimum values of thermal performance, including the crystallinity, melting point, and melting range were observed when the cables were annealed at 100, 105, and 105 °C for the inner, middle and outer positions, respectively. The optimum values of the electrical conductivity and dielectric breakdown strength were reached at annealing temperatures of 95 or 100 °C for the inner and middle position, respectively, and at 105 °C for the outer position.

2) Thermal annealing at these temperatures of the three cables for hundreds of hours did not cause further breakage in the molecular chains.

3) In terms of cable structure, 95 °C is the optimum point for the two retired cables since the cables annealed at this point exhibit the optimum electrical conductivity and dielectric breakdown strength, which significantly enhances the thermal performance.

4) As far as the results for the three cables are concerned, heat treatment applied through the simulation of cable operation would be a feasible method to rejuvenate retired cables.

Further research will be conducted on long cables, with the cable terminals and joints used to build an experimental cable line. High voltage and current will be applied, and the annealing process will be performed. The feasibility of retired cable rejuvenation by heat treatment will be further verified.

REFERENCES

[1] G. Wypych, *Handbook of Polymers*, 2013.
[2] F. Aras, V. Alekperov, N. Can, and H. Kirkici, "Aging of 154 kV underground power cable insulation under combined thermal and electrical stresses," *IEEE Elect. Insul. Mag.*, vol. 23, no. 5, pp. 25–33, Sep. 2007.
[3] W. Li, J. Li, X. Wang, S. Li, G. Chen, J. Zhao, and B. Ouyang, "Physicochemical origin of space charge dynamics for aged XLPE cable insulation," *IEEE Trans. Dielectr. Electr. Insul.*, vol. 21, no. 2, pp. 809–820, Apr. 2014.
[4] N. Hirano, T. Tsujimura, N. Shimizu, and K. Horii, "Diagnosis of the aged XLPE cable using frequency and temperature characteristics of tan δ II," in *Proc. 21st Symp. Electr. Insulating Mater.*, Sep. 1998, pp. 179–182. [Online]. Available: https://ieeexplore.ieee.org/stamp/stamp.jsp?tp=&arnumber=763468
[5] W. Liming, H. Jingzhou, and C. Changlong, "Diagnosis of XLPE cable insulation using velocity of electromagnetic wave," *High Voltage Eng.*, vol. 37, no. 12, pp. 2984–2989, 2011.
[6] E. Gulski, F. Wester, J. Smit, P. Seitz, and M. Turner, "Advanced partial discharge diagnostic of MV power cable system using oscillating wave test system," *IEEE Electr. Insul. Mag.*, vol. 16, no. 2, pp. 17–25, Mar. 2000.
[7] H. Ghorbani, M. Saltzer, F. Abid, and H. Edin, "Effect of heat-treatment and sample preparation on physical properties of XLPE DC cable insulation material," *IEEE Trans. Dielectr. Electr. Insul.*, vol. 23, no. 5, pp. 2508–2516, Oct. 2016.
[8] Y. Ren, H. Zou, S. Wang, J. Liu, D. Gao, C. Wu, and S. Zhang, "Effect of annealing on microstructure and tensile properties of polypropylene cast film," *Colloid Polym. Sci*, vol. 296, no. 1, pp. 41–51, Jan. 2018.
[9] Y. Xu, P. Luo, M. Xu, and T. Sun, "Investigation on insulation material morphological structure of 110 and 220 kV XLPE retired cables for reusing," *IEEE Trans. Dielectr. Electr. Insul.*, vol. 21, no. 4, pp. 1687–1696, Aug. 2014.
[10] C. Katz and W. Zenger, "Service aged 69 and 115 kV XLPE cables," *IEEE Trans. Power Del.*, vol. 14, no. 3, pp. 685–689, Jul. 1999.
[11] G. Mazzanti, "Analysis of the combined effects of load cycling, thermal transients, and electrothermal stress on life expectancy of high–voltage AC cables," *IEEE Trans. Power Del.*, vol. 22, no. 4, pp. 2000–2009, Oct. 2007.
[12] Y. Xie, G. Liu, Y. Zhao, L. Li, and Y. Ohki, "Rejuvenation of retired power cables by heat treatment," *IEEE Trans. Dielectr. Electr. Insul.*, vol. 26, no. 2, pp. 668–670, Apr. 2019.
[13] Y. Xie, Y. Zhao, G. Liu, J. Huang, and L. Li, "Annealing effects on XLPE insulation of retired high–voltage cable," *IEEE Access*, vol. 7, pp. 104344–104353, 2019.
[14] Y. Song and Q. Zheng, "Influence of annealing on conduction of high-density polyethylene/carbon black composite," *J. Appl. Polym. Sci.*, vol. 105, no. 2, pp. 710–717, Jul. 2007.
[15] A. Saffar, A. Ajji, P. J. Carreau, and M. R. Kamal, "The impact of new crystalline lamellae formation during annealing on the properties of polypropylene based films and membranes," *Polymer*, vol. 55, no. 14, pp. 3156–3167, Jun. 2014.
[16] D. Ferrer-Balas, M. Maspoch, A. Martinez, and O. Santana, "Influence of annealing on the microstructural, tensile and fracture properties of polypropylene films," *Polymer*, vol. 42, no. 4, pp. 1697–1705, Feb. 2001.
[17] H. Bai, H. Deng, Q. Zhang, K. Wang, Q. Fu, Z. Zhang, and Y. Men, "Effect of annealing on the microstructure and mechanical properties of polypropylene with oriented shish-kebab structure," *Polym. Int.*, vol. 61, no. 2, pp. 252–258, Feb. 2012.
[18] B. Wunderlich, *Thermal Analysis of Polymeric Materials*. Springer, 2005, ch. 2.

[19] N. Hozumi, M. Ishida, T. Okamoto, and H. Fukagawa, "The influence of morphology on electrical tree initiation in the polyethylene under AC and impulse voltages," in *Proc. 2nd Int. Conf. Properties Appl. Dielectric Mater.*, Beijing, China, Jan. 2003, pp. 481–485.
[20] K. Gasparyan, V. Borokhonovskii, L. Sevast'yanov, R. Mirzoyev, and V. Baranov, "The melting temperature range of polymers," *Polym. Sci. U.S.S.R.*, vol. 18, no. 3, pp. 628–632, Jan. 1976.
[21] D. V. Rees and D. C. Bassett, "On the formation of extended-chain lamellae in polyethylene," *J. Polym. Sci. B, Polym. Lett.*, vol. 7, no. 4, pp. 273–280, Apr. 1969.
[22] J. Fothergill, G. Montanari, G. Stevens, C. Laurent, G. Teyssedre, L. Dissado, U. Nilsson, and G. Platbrood, "Electrical, microstructural, physical and chemical characterization of HV XLPE cable peelings for an electrical aging diagnostic data base," *IEEE Trans. Dielectr. Electr. Insul.*, vol. 10, no. 3, pp. 514–527, Jun. 2003.
[23] Y. Murakami, M. Nemoto, S. Okuzumi, S. Masuda, M. Nagao, N. Hozumi, Y. Sekiguchi, and Y. Murata, "DC conduction and electrical breakdown of MgO/LDPE nanocomposite," *IEEE Trans. Dielectr. Electr. Insul.*, vol. 15, no. 1, pp. 33–39, 2008.
[24] M. Araoka, H. Yoneda, and Y. Ohki, "Dielectric breakdown of new type polymerized polyethylene using a single-site catalyst," *IEEE Trans. Dielectr. Electr. Insul.*, vol. 6, no. 3, pp. 326–330, Jun. 1999.
[25] Y. L. Chong, G. Chen, I. L. Hosier, A. S. Vaughan, and Y. F. F. Ho, "Heat treatment of cross-linked polyethylene and its effect on morphology and space charge evolution," *IEEE Trans. Dielectr. Electr. Insul.*, vol. 12, no. 6, pp. 1209–1221, Dec. 2005.
[26] J. Gulmine and L. Akcelrud, "FTIR characterization of aged XLPE," *Polym. Test.*, vol. 25, no. 7, pp. 932–942, Oct. 2006.

YUE XIE received the B.Eng. degree in electrical engineering from Wuhan Polytechnic University, Wuhan, China, in 2013. He is currently pursuing the Ph.D. degree in electrical engineering with the South China University of Technology, Guangzhou, China. His research interests include degradation mechanism of polymer dielectric materials and aging assessment of XLPE cable.

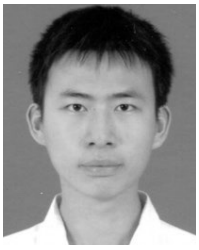

YIFENG ZHAO received the B.Eng. degree in electrical engineering from Qingchuan University, Wuhan, China, in 2017. He is currently pursuing the M.Eng. degree in electrical engineering with the South China University of Technology, Guangzhou, China. His research interests include degradation mechanism of polymer dielectric materials and aging assessment of XLPE cable.

SHUZHEN BAO received the B.Eng. degree in electrical engineering from Fuzhou University, Fuzhou, China, in 2019. She is currently pursuing the M.Eng. degree in electrical engineering with the South China University of Technology, Guangzhou, China. Her current research focuses on the interfacial pressure of the cable accessory.

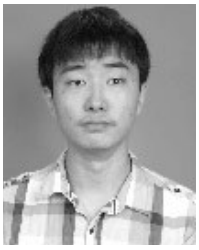

PENGYU WANG received the B.Sc. (Eng.) degree in electrical engineering from the South China University of Technology, Guangzhou, China, in 2016, where he is currently pursuing the Ph.D. degree in electrical engineering. His research interests include ampacity assessment and fault diagnosis of power cable.

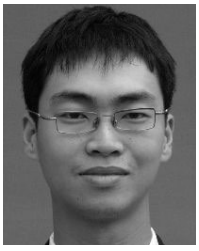

JIASHENG HUANG received the B.Eng. degree in electrical engineering from the Guangdong University of Technology, Guangzhou, China, in 2004. Since 2004, he has been an Engineer with Guangzhou Power Supply Company, Ltd., Guangzhou, China. His research interest is failure diagnose of transmission cables.

GANG LIU received the B.Eng., M.Eng., and Ph.D. degrees in electrical engineering from Xi'an Jiaotong University, Xi'an, China, in 1991, 1994, and 1998, respectively. He is currently an Associate Professor with the School of Electric Power, South China University of Technology, Guangzhou, China. His research interests include ampacity assessment and fault diagnosis of electrical equipments and lightning protection of transmission line.

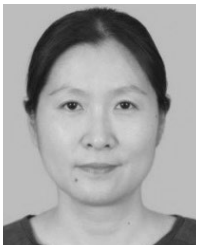

YANPENG HAO (Member, IEEE) was born in Hebei, China, in 1974. She received the M.Sc. and Ph.D. degrees in electrical engineering from Xi'an Jiaotong University, China, in 1998 and 2003, respectively. She is currently a Professor with the South China University of Technology, China. Her major research fields are insulation condition monitoring and life evaluation of electrical power equipment, insulation performance of UHV/EHV Transmission lines under lighting, icing, and pollution.

LICHENG LI received the B.Eng. degree in electrical engineering from Tsinghua University, China, in 1967. He is currently an Academician of the Chinese Academy of Engineering and a Professor and the Ph.D. Supervisor with the South China University of Technology. He is also the Secretary of the Expert Committee, China Southern Power Grid.